Article title:

PI3Kδ inhibition potentiates glucocorticoids in B-ALL by decreased receptor phosphorylation and enhanced gene regulation

Short title:

PI3Kδ inhibition enhances glucocorticoids in B-ALL

Authors:

Jessica A.O. Zimmerman[1,2], Mimi Fang[2,3], and Miles A. Pufall[2,3]

Affiliations:

[1]Division of Pediatric Hematology/Oncology, Stead Family Department of Pediatrics, Carver College of Medicine, University of Iowa, Iowa City, IA

[2]Holden Comprehensive Cancer Center, University of Iowa, Iowa City, IA

[3]Department of Biochemistry and Molecular Biology, Carver College of Medicine, University of Iowa, Iowa City, IA

Corresponding author:

Miles Pufall, PhD
Carver College of Medicine
University of Iowa
51 Newton Rd, 4-430 BSB
Iowa City, IA 52242
Email: miles-pufall@uiowa.edu
Phone: (319) 384-1820
Fax: (319) 335-9570

Abstract word count: 208

Text word count: 3998

Reference count: 41

Figure count: 6

Table count: 1

Scientific category: Lymphoid Neoplasia

KEY POINTS

1) Idelalisib potentiates glucocorticoids in B-ALL in part by reducing GR phosphorylation and enhancing gene regulation
2) Inhibition of tissue-restricted PI3Kδ likely allows durable potentiation expressly in B-ALL, even as the glucocorticoid is cleared

ABSTRACT

Glucocorticoids, including dexamethasone and prednisone, are key components of therapy for B-lymphoblastic leukemia (B-ALL) that work through the glucocorticoid receptor (GR). However, glucocorticoids are not effective for all patients, leading to poor outcomes, and their use is hampered by undesirable toxic effects. We have shown that inhibition of PIK3δ, the leukocyte-restricted delta isoform of the catalytic subunit of phosphoinositide 3-kinase, is a promising way to specifically enhance the effect of glucocorticoids in B-ALL, with the potential to improve outcomes without increasing toxicities. Here, we show that the PI3Kδ inhibitor idelalisib potentiates both prednisolone and dexamethasone in B-ALL cell lines and most primary patient specimens, particularly at sub-saturating doses of glucocorticoids. Potentiation is explained in part by a widespread enhancement of glucocorticoid-induced gene regulation, including of effector genes that drive B-ALL cell death. Idelalisib causes a reduction in phosphorylation of GR at S203 and S226, and ablation of these phospho-acceptor sites enhances glucocorticoid potency. Because phosphorylation of S226 inhibits GR DNA binding, we propose that PI3Kδ inhibition improves glucocorticoid efficacy in B-ALL in part by decreasing inhibitory GR phosphorylation and enhancing DNA binding and downstream gene regulation. These studies provide a pre-clinical and mechanistic rationale for clinical application of PI3Kδ inhibitors in combination with glucocorticoids for treatment of B-ALL.

INTRODUCTION

Glucocorticoids, including dexamethasone and prednisone, are the cornerstone of chemotherapy regimens for B-lymphoblastic leukemia (B-ALL), the most common childhood cancer[1]. Response to glucocorticoid therapy alone predicts overall outcomes for patients with B-ALL[2,3]. Therefore, enhancing endogenous GR activity remains an attractive way to improve outcomes. Glucocorticoids work through the glucocorticoid receptor (GR), a ligand-activated transcription factor that regulates genes inducing B-ALL cell death. Regulation of apoptotic gene programs, including suppression of *BCL2* and enhancement of *BCL2L11*[4,5], and suppression of B-cell developmental genes[6] are both important for glucocorticoid response. Due to serious short- and long-term toxicities, the use of more potent or higher dose glucocorticoids is not possible[7-9]. Tissue-specific enhancement of GR activity could lead to better outcomes in patients with less glucocorticoid sensitive B-ALL without increasing the accompanying off-tumor effects and may allow reduced glucocorticoid doses. We therefore sought to enhance glucocorticoid activity, particularly of prednisone, which is better tolerated than dexamethasone, by targeting B-ALL-restricted proteins.

Among the most promising is PI3Kδ (*PIK3CD*), a key component of the B-cell receptor (BCR) and interleukin-7 receptor (IL-7R) pathways, which we identified using functional genomics[6,10]. PI3Kδ activates multiple pathways, including Ras/MAPK, impairing glucocorticoid-induced cell death in B-ALL. The leukocyte-restricted expression of PI3Kδ[11] makes it an appealing target to enhance glucocorticoid potency in B-ALL without increasing off-tumor effects. The combination of idelalisib, a PI3Kδ inhibitor,

and dexamethasone synergistically induces B-ALL cell death. However, these studies were performed in in a limited number of specimens[6] making it unclear whether idelalisib and glucocorticoids, including prednisone, would be synergistic in most patients.

Our previous data suggested that idelalisib potentiates glucocorticoid activity by enhancing regulation of select genes[6]. We identified a set of effector genes, regulated by glucocorticoids, that contribute to glucocorticoid-induced cell death. Idelalisib enhanced regulation of only some effector genes, with differing effects in three B-ALL cell lines. A systematic analysis of idelalisib's effect on glucocorticoid gene regulation in primary specimens would elucidate how idelalisib potentiates glucocorticoid activity.

The potentiation of glucocorticoids by PI3Kδ inhibition could be a result of blocking phosphorylation of GR. Phosphorylation of GR by the BCR/Ras/MAPK pathway can modulate the receptor's activity, although the effect is cell-type and gene specific[12-14]. Many kinases, including the terminal kinase in the Ras/MAPK pathway, ERK2 (MAPK1), phosphorylate GR at multiple sites, including S203, S211 or S226[12,13] and is associated with glucocorticoid resistance[15]. Treatment of B-ALL cells with idelalisib is accompanied by a decrease in phosphorylation of GR at S203[6]. However, it is unclear which sites of ERK2 phosphorylation directly affect GR activity in B-ALL.

Here we show that, as with dexamethasone[6], idelalisib synergistically enhances prednisolone-induced cell death in B-ALL cell lines and most primary patient specimens, particularly at concentrations near the EC50 of dexamethasone and prednisolone. We show that this potentiation is the result of global enhancement of glucocorticoid-induced gene regulation rather than select cell-death genes. Consistent with this global effect, we show that phosphorylation of S226 decreases the affinity of GR for DNA, suggesting that idelalisib enhances GR function in part by enhancing DNA binding.

METHODS

Cell viability assays

Two B-ALL cell lines (NALM6 and RS4;11) and two NALM6 phospho-GR mutants (GR-S203A and GR-S226A) were tested with combinations of prednisolone (Acros Organics, #449470250) and the PI3Kδ inhibitor idelalisib (Gilead, Lot 5). Viability was measured using PrestoBlue (ThermoFisher, A13262). Synergy, meaning a greater than additive response to combination treatment, was evaluated using SynergyFinder 2.0 with the Bliss synergy model and replicate measurements[16].

Primary patient specimens from children and adolescents with newly diagnosed or relapsed B-ALL were obtained after receiving informed consent (University of Iowa IRB protocol #201707711). Cells were isolated by Histopaque density gradient separation prior to testing.

NALM6, SUP-B15, and RCH-ACV cells were tested with dexamethasone (Sigma, D4902-1g) in combination with ERK1/2 inhibitor SCH772984 (SelleckChem, #S7101).

Gene expression analysis of NALM6 cells and primary specimens

NALM6 cells were treated with vehicle, dexamethasone (5 nM or 50 nM), idelalisib (250 nM), or combination dexamethasone (both concentrations) and idelalisib. Seven primary patient specimens (MAP010, MAP014, MAP015, MAP016, MAP019, MAP020, MAP031) were treated with vehicle, dexamethasone (25 or 50 nM), prednisolone (25 or 50 nM), idelalisib (500 nM), combinations of dexamethasone and idelalisib, or combinations of prednisolone and idelalisib. RNA was extracted after

24-hour treatment using the miRNeasy Mini Kit (Qiagen, #217004). RNA quality was assessed using an Agilent Bioanalyzer. Libraries were sequenced by the Iowa Institute of Human Genetics Genomics Division. Sequencing data was processed using R/Bioconductor and DESeq2[17] with RUVSeq[18]. Code for the analysis is available in supplemental files (**Supplemental files 1 and 2**).

Protein expression and purification

The human GR AF1-DBD (27-506) polypeptide, which contains most of the N-terminal AF1 region and the DNA Binding Domain (DBD), was expressed and purified as described for the DBD alone[19]. ERK2 was expressed and purified as described[20].

Phosphorylation of GR-AF1-DBD and purification

GR-AF1-DBD was phosphorylated by ERK2 for 30 minutes at 30˚C. We used a higher ratio of ERK2 to GR-AF1-DBD (100:1) to favor more highly phosphorylated GR-AF1-DBD and a lower ratio (10,000:1) to favor addition of fewer phosphates. GR-AF1-DBD phosphorylated species were separated on a 5/5 MonoQ column (Cytiva), run over a size exclusion column (Cytiva, Superdex 200), concentrated, snap frozen, and stored at -80˚C.

Mass Spectrometry

GR-AF1-DBD +/- phosphorylation (5 µg) samples were reduced, alkylated, digested with trypsin, and purified with C18 stage tips (Pierce, #87781)[21,22]. Peptides were then separated by LC and analyzed on a QExactive HF Orbitrap (ThermoFisher) mass spectrometer. Peptides were matched to human proteins and quantified using Proteome Discoverer (ThermoFisher). Fully phosphorylated GR and singly phosphorylated GR were compared to unmodified GR-AF1-DBD using Scaffold 5.1.2 (Proteome Software Inc.). Phospho-fragment frequencies were calculated and compared to the control to determine the level of phosphorylation at each site.

Electrophoretic Mobility Shift Assays (EMSA)

The dissociation constants for unmodified and phosphorylated GR-AF1-DBD fragments were measured by electrophoretic mobility shift assay (EMSA) as described[19] using a consensus GR site (5'-GTAC**GGAACA**TCG**TGTACT**GTAC – 3').

Phospho-GR western blotting

NALM6 cells were treated with vehicle, dexamethasone (5 nM or 1 µM), idelalisib 250 nM, or dexamethasone plus idelalisib for 24 hours. Western blotting was performed as described[6] using GR-S203P or GR-S226P rabbit polyclonal antibody (generously provided by the Garabedian Lab) or purified GR IA-1[6]. Changes in GR phosphorylation were determined as the ratio of phospho-GR to total GR compared to controls.

Phospho-GR mutants by CRISPR

Cas9-RNPs were transfected into cells by electroporation (SF Cell Line 4D-Nucleofector™ X Kit S (Lonza, #V4XC-2032). After 48-72 hours, editing efficiency was checked by T7EI digest (IDT, #1075931). Cells were single-cell sorted (Becton Dickinson Aria II) into 96 well plates. Positive clones were identified by extracting genomic DNA, PCR amplifying the region, Sanger sequencing of control, experimental, and reference PCR products, and analyzing by TIDER[23].

Data sharing statement

RNA sequencing data are available at Gene Expression Omnibus (NALM6 cells: GSE215385) and dbGaP (patient specimens: phs003085.v1.p1). For other original data, contact miles-pufall@uiowa.edu.

Additional details are available in the supplement.

RESULTS

Inhibition of PI3Kδ increases prednisolone sensitivity in B-ALL cell lines and primary patient specimens

To determine whether idelalisib synergizes with prednisolone to induce B-ALL cell death similar to dexamethasone, we titrated both into two B-ALL cell lines (RS4;11, NALM6) and measured viability. RS4;11 cells were more sensitive to prednisolone (EC50 = 25 nM) than NALM6 cells (EC50 = 80 nM). When combined with idelalisib, RS4;11 and NALM6 cells exhibited additivity based on overall Bliss score (RS4;11: 5.826 ± 0.88; NALM6: 3.055 ± 0.56), but both were highly synergistic at some prednisolone concentrations (peak Bliss score 23.30 for RS4;11; 23.79 for NALM6). The idelalisib concentration at peak synergy is similar in both cell lines (~1.5 µM), but the prednisolone concentration is around half of the EC50 (RS4;11 ~10 nM; NALM6 ~40 nM) (**Figure 1A-B**). This suggested that idelalisib is synergistic at prednisolone concentrations near the EC50 and lower than expected clinical concentrations (~4.5 µM for 60 mg/m^2 prednisone dose).

We then evaluated prednisolone/idelalisib synergy by testing 20 primary B-ALL specimens (**Table 1**). Most primary specimens were sensitive to prednisolone (EC50 = 6.5-71 nM). Two specimens were less sensitive (MAP010: 105 nM; MAP021: 250 nM) and another (MAP020) was resistant. We then compared the EC50 of each specimen to the viability of the specimen at the maximum concentration of prednisolone (10 µM) (**Figure 1C**). Fourteen specimens had <30% viability, with the majority (12/14) from patients with negative end of induction minimal residual disease (MRD). Of the six specimens with >50% viability, four were MRD positive, one was MRD negative, and one was unknown. Thus, consistent with the literature[2,24], we find that prednisolone response correlates with patient response, particularly with respect to reduction in viability (**Supplemental Figure 1**).

To account for both prednisolone EC50 and viability of each specimen, we calculated area under the curve (AUC) and compared these to overall and peak Bliss scores. Although no correlation reached statistical significance, a trend emerged with higher prednisolone AUC associated with lower overall and peak Bliss scores (R = -0.34 and -0.37, respectively; **Figure 1D-E**). This suggests that lower glucocorticoid sensitivity may be associated with increased idelalisib synergy.

We next sought to determine whether National Cancer Institute (NCI) risk grouping or cytogenetic features correlated with synergy. An additive response of idelalisib with prednisolone was observed in most (18/20) specimens based on overall Bliss score. Overall antagonism was evident in the two remaining specimens with notable cytogenetic features – MAP010 (overall Bliss score -10.6 ± 1.1) with near haploid cytogenetics, and MAP018 (overall Bliss score -15.4 ± 2.4) with *BCR::ABL1*. Fourteen specimens exhibited a peak synergistic area (**Figure 1F-I, Supplemental Figure 2**). As in the cell lines, the peak synergistic area is near the prednisolone EC50 in all specimens except for three specimens with >50% viability (MAP012, MAP020, MAP025) and the relapsed B-ALL specimen (MAP019). Unlike cell line models, peak synergy in primary patient specimens does not occur at a consistent idelalisib concentration. We were also able to treat seven specimens with dexamethasone in combination with

idelalisib, producing similar results (**Supplemental Figure 3**). Thus, synergy between idelalisib and glucocorticoids was evident across NCI risk and cytogenetic groups, though not in every specimen.

PI3Kδ inhibition induces global enhancement of glucocorticoid-induced gene regulation in NALM6 cells

To understand the mechanism of idelalisib-enhanced cell death, we measured changes in gene regulation with dexamethasone and idelalisib in NALM6 cells by RNA-seq. We first identified differentially regulated genes (adjp ≤ 0.01) in response to low dexamethasone (5 nM, ~EC50), high dexamethasone (50 nM), idelalisib (250 nM), and the combination of low and high dexamethasone with idelalisib. Idelalisib induced up- and down-regulation of 418 genes (**Figure 2A**). Low dexamethasone induced regulation of fewer genes (649) than high dexamethasone (3779). The combination caused a greater than additive effect in the number of genes regulated, particularly with low dexamethasone (2398 combination vs. 1067 separately) compared to high dexamethasone (4965 combination vs. 4197 separately). This indicates that the combination either induces regulation of new genes relative to either drug alone or enhances dexamethasone-induced gene regulation.

To distinguish between these models, we performed linear regression on genes regulated by dexamethasone plus idelalisib (**Figure 2B-C**). For genes regulated by low dexamethasone, idelalisib significantly enhances both up-regulation ($p = 5e^{-9}$) and down-regulation ($p = 1e^{-7}$) with an average enhancement of 18% ($p < 2e^{-12}$). There is a more modest, but significant, effect of idelalisib with high dexamethasone (3%, $p = 1.6e^{-5}$). This supports the model that idelalisib better enhances gene regulation at glucocorticoid concentrations closer to the EC50 than at high concentrations.

To determine whether adding idelalisib causes regulation of new genes, we incorporated an interaction term in the differential gene expression model. Of 2398 genes regulated by low dexamethasone plus idelalisib, only 18 exhibited a greater than additive effect. Of 4965 genes regulated by high dexamethasone and idelalisib, 72 showed a greater than additive effect. This indicates that a minority of genes are synergistically or newly regulated by the combination, which we evaluate below.

Idelalisib potentiates glucocorticoid-induced cell death by generally enhancing glucocorticoid gene regulation

We first sought to determine whether idelalisib potentiates regulation of effector genes. We identify effector genes by integrating gene regulation data with the results of two large-scale gene knockdown screens in NALM-6 cells previously performed by our lab to identify genes impacting glucocorticoid-mediated cell death[6,10] (**Figure 2D**). Positive effectors are genes that contribute to dexamethasone-induced cell death (as measured in the screens) and are upregulated by dexamethasone, thereby enhancing cell death. Negative effectors are genes which impair dexamethasone-induced cell death but are down-regulated by dexamethasone, also enhancing cell death. Our highest confidence effector genes are significant in both versions of the screen[6,10] ($p < 0.01$).

As with most dexamethasone-regulated genes, idelalisib significantly enhances up- and down-regulation of effector genes with low dexamethasone (19%, $p = 0.007$) but only sporadically enhances genes with high dexamethasone (**Figure 2E**). Only *LSS* and *MED13L* were newly or synergistically regulated upon addition of idelalisib. This indicates that the primary mechanism of glucocorticoid potentiation by idelalisib is global enhancement of gene regulation.

BMF is a key effector of glucocorticoid-induced cell death in NALM6 cells

NALM6 effector genes are different than the overall effector genes reported previously[6] in some key ways (**Supplemental Table 1**). Of the NALM6 positive effectors (88 genes), most were effectors from previous studies[6,10], including GR, GR coregulators (e.g., *NCOA1, NCOR2*), and the pro-apoptotic *BCL2L11*. Similarly, most key NALM6 negative effectors (148 genes) were shared, including anti-apoptotic *BCL2,* RNA-binding protein *MBNL1,* and B-cell development genes (e.g., *CD19*, *LEF1*, *PAX5*, and importantly, *PIK3CD*, which encodes the target of idelalisib). However, *BMF*, not *BCL2L11*, appears to be the most important dexamethasone-induced pro-apoptotic gene in NALM6 cells. *BMF* has a stronger dexamethasone sensitivity phenotype (0.4 vs. 0.26) and is more strongly regulated (log2 fold change 4.2 vs. 1.1) compared to *BCL2L11* in NALM6 cells. *BMF* is not as strongly regulated by glucocorticoids in all primary B-ALL specimens, suggesting that glucocorticoid-driven apoptosis programs can vary.

PI3Kδ inhibition enhances prednisolone-induced gene regulation in primary patient specimens

To test whether idelalisib enhances glucocorticoid potency by globally enhancing gene regulation in a more clinically relevant context, we performed RNA-seq in seven freshly isolated primary B-ALL specimens. Because the glucocorticoid sensitivity of each specimen was unknown at the time of treatment, a relatively high standard dexamethasone concentration (25 or 50 nM) was used. The same prednisolone concentration was used, which is 6-10-fold less potent than dexamethasone. Dexamethasone regulated 1346 genes (adjp ≤ 0.01), and prednisolone regulated fewer (99). Idelalisib alone regulated only 7 genes and did not enhance the gene-regulating effects of dexamethasone or prednisolone (**Supplemental Figure 4**). This is likely because two specimens (MAP010, MAP020) are resistant to glucocorticoids (>50% viability at 10 µM prednisolone), exhibiting regulation of very few genes (dexamethasone 41, prednisolone 8, adjp < 0.01).

We therefore tested whether idelalisib enhanced regulation in glucocorticoid-responsive specimens (MAP014, MAP015, MAP019, MAP016, MAP031). In these specimens, dexamethasone induced regulation of 1951 genes and prednisolone 146 genes (**Figure 3A**). Idelalisib alone only regulated 6 genes. These specimens showed enhanced gene regulation upon addition of idelalisib to prednisolone (**Figure 3B**), similar to the combination of idelalisib and low dexamethasone in NALM6 cells. However, idelalisib did not enhance gene regulation with dexamethasone (**Supplemental Figure 4**). Effector genes in these specimens also showed similar patterns of enhanced expression as NALM6 cells (**Supplemental Figure 5**).

We then evaluated whether idelalisib better enhanced gene regulation in specimens that responded synergistically (MAP015, MAP019) compared to those that responded additively (MAP014, MAP031) at the treatment concentrations. Counterintuitively, dexamethasone and prednisolone regulated more genes in additive compared to synergistic specimens (dexamethasone 6195 vs. 4015; prednisolone 1447 vs. 1115; adjp ≤ 0.01). Idelalisib alone regulated genes in additive specimens (298) but few in synergistic specimens (10) (**Figure 3C-D**). When comparing glucocorticoid-regulated genes shared by both groups, additive specimens demonstrated stronger gene regulation with dexamethasone, and to a lesser extent with prednisolone, compared to synergistic specimens (**Figure 3E-F**). Because additive specimens were also more sensitive to prednisolone based on viability (MAP014 13%, MAP031 8%) compared to synergistic specimens (MAP015 25%, MAP019 27%), we hypothesized that synergistic specimens may be more amenable to glucocorticoid potentiation than additive specimens.

To evaluate this model, we examined how the addition of idelalisib changed glucocorticoid regulation of genes in the additive and synergistic specimens. Idelalisib did not enhance regulation of genes in either

the additive or synergistic specimens compared to dexamethasone alone (**Figure 3G-H**), consistent with NALM6 high dexamethasone treatments. Counter to the model, idelalisib did enhance prednisolone gene regulation in additive specimens (**Figure 3I**), but not in synergistic specimens (**Figure 3J**), possibly due a stronger effect on gene regulation by idelalisib alone in additive specimens. We identified effector genes in the additive and synergistic specimens, and none were specifically regulated in the synergistic specimens to explain synergy (**Supplemental Table 2**). This lack of a clear pattern of enhanced gene regulation in potentiated specimens may be because enhanced gene regulation appears to be highly concentration dependent. Because we prioritized testing freshly isolated specimens, precluding optimization of drug concentrations to achieve maximum synergy in each specimen, the doses used may mask differences in enhancement in additive and synergistic specimens.

GR is phosphorylated by ERK2 at six sites, most prominently S226

To understand the mechanism of idelalisib-enhanced gene regulation, we examined how idelalisib affects GR phosphorylation. We previously mapped MAPK1/ERK2, a key kinase in B-ALL transformation[25], downstream of PI3Kδ in the B-cell receptor pathway[6]. To test this, we measured synergy between an ERK1/2 inhibitor (SCH772984) and dexamethasone in three B-ALL cell lines (NALM6, SUP-B15, and RCH-ACV). The overall and peak Bliss scores were consistent with combination dexamethasone and idelalisib (**Supplemental Figures 6-8**), supporting the model that ERK2 lies downstream of PI3Kδ.

We then examined how direct phosphorylation of GR by ERK2[26] affects its activity. To identify relevant sites of ERK2 phosphorylation on GR, we expressed and purified a fragment of GR composed of the N-terminus and DNA binding domain (GR-AF1-DBD), which recapitulates the binding of full-length GR and retains the most commonly phosphorylated sites, and phosphorylated it with ERK2. This resulted in a hazy band shifted upward on an SDS-PAGE gel, indicating that GR-AF1-DBD was phosphorylated but as a mixture of species. We separated the differently phosphorylated species using strong anion exchange (MonoQ) into a high and low mobility species (**Figure 4A**). Interestingly, the highly phosphorylated form of GR-AF1-DBD (GR-6P) eluted in the same volume as the unmodified GR-AF1-DBD over a size exclusion column, but the mono-phosphorylated form (GR-1P) eluted at a later volume. This indicates that GR-1P adopts a more compact conformation than the unmodified or GR-6P species (**Figure 4B**).

Phosphopeptide mapping by mass spectrometry of GR-6P indicated that it is likely a mixture of species with six predominant sites of phosphorylation (**Figure 4C**). Two sites (S203 and S226) were previously reported as sites of ERK2 phosphorylation, but the others are rarely observed (S45, S267, and T288) or previously unreported (S148). The low mobility species was predominantly phosphorylated at a single site - S226 (GR-1P).

We tested the effect of phosphorylation on GR activity by measuring the DNA-binding affinity by electrophoretic mobility shift assay (EMSA) for a consensus GR site (5'-GTAC**GGAACA**TCG**TGTACT**GTAC – 3'). The affinity of GR-6P was modestly (50%) but significantly ($p = 0.004$) inhibited compared to the unmodified GR. Surprisingly, GR-1P was both substantially (~3x) and significantly ($p < 0.0001$) inhibited compared to unmodified and GR-6P (**Figure 4D**). This indicates that phosphorylation of GR by ERK2 not only inhibits GR binding to DNA, but the pattern of phosphorylation can have an important effect, with S226 phosphorylation as a key modification for directly regulating GR affinity.

Blocking phosphorylation of GR S203 or S226 increases glucocorticoid sensitivity and contributes to idelalisib-induced glucocorticoid potentiation

To validate the importance of S226 phosphorylation, we studied its effect on native GR activity in NALM6 cells. We first performed western blots (**Figure 5A**) on S226 along with S203, which has been shown to inhibit GR function when phosphorylated[27,28]. Consistent with previous studies showing reduced S203 phosphorylation at high (1 µM) dexamethasone[6], treatment with idelalisib appeared to reduce low (5 nM) dexamethasone-induced phosphorylation of S203, though not significantly ($p = 0.36$) (**Figure 5B**). In contrast, S226 phosphorylation significantly decreased with idelalisib alone ($p = 0.01$) (**Figure 5C**), suggesting that idelalisib can affect phosphorylation of GR at both S203 and S226.

To test the importance of these sites, we generated phospho-acceptor mutants (GR-S203A and GR-S226A) in NALM6 cell lines using CRISPR. Blocking phosphorylation at S203 (**Figure 5D**) and S226 (**Figure 5E**) increased the sensitivity of NALM6 cells to prednisolone (EC50s: wild-type ~80 nM, GR-S203A ~70 nM, GR-S226A ~60 nM), indicating that phosphorylation at either site attenuates GR activity.

Interestingly, when treated with idelalisib and prednisolone, the GR-S203A clones had similar overall Bliss scores to wild-type NALM6 cells, but peak Bliss scores shifted towards lower idelalisib concentrations (**Figure 5F**). The GR-S226A clones showed decreased overall Bliss scores compared to wild-type NALM6 cells, but peak Bliss scores remained at similar idelalisib concentrations (**Figure 5G**). This suggests that S203 and S226 both contribute to glucocorticoid potentiation with differing and incomplete effects, indicating that other PI3Kδ targets also impact idelalisib-induced glucocorticoid potentiation.

DISCUSSION

Our previous work[6] identified PI3Kδ inhibition as a promising strategy for glucocorticoid potentiation in B-ALL for two main reasons: 1) small molecule inhibitors against PI3Kδ are available, and 2) *PIK3CD* expression is restricted to leukocytes, which could restrict glucocorticoid potentiation to these cells. In this work, we show that PI3Kδ inhibition using idelalisib potentiates both dexamethasone and prednisolone. This could be particularly beneficial for patients with high-risk B-ALL who receive prednisone due to excess toxicity with dexamethasone[29] and are more prone to relapse.

Our data indicates that idelalisib augments the potency of glucocorticoids in B-ALL and is most synergistic near the glucocorticoid EC50. PI3Kδ inhibition with idelalisib directly enhances the gene-regulatory function of GR, in part by reducing phosphorylation at S203 and S226. This is consistent with other studies showing that S203 phosphorylation inhibits GR function[27,28] and S226 phosphorylation inhibits activation of transcription with glucocorticoids[13]. Here we link S226 phosphorylation to inhibition of DNA binding, attenuating the regulation of most GR-regulated genes (**Figure 6**).

Because synergy with idelalisib remains in GR-S203A or GR-S226A cells, other phosphorylation sites on GR or non-GR targets of ERK2 likely contribute. Here we identify 6 sites of ERK2 phosphorylation on GR, including one (S148) that has not been reported to be phosphorylated by any kinase. Testing each site individually and in combination is now feasible using CRISPR. However, isolation of homogenously phosphorylated species is more challenging, likely preventing *in vitro* study and highlighting the novelty of our work on S226. ERK2 can phosphorylate hundreds of other proteins[30], including effectors in the BCL2 apoptosis pathway[31] and PAX5[32]. Our functional genomic studies enabled us to scrutinize NALM6

cells, revealing that ERK2 likely impacts glucocorticoid-regulated, BCL2-driven apoptosis differently. NALM6 cells favor BMF rather than BCL2L11, which is favored in other backgrounds, necessitating the evaluation of ERK2 in multiple types of B-ALL.

PI3Kδ inhibition may also have effects separate from ERK2. For example, the PI3K/AKT pathway phosphorylates and inhibits FOXO proteins, which also upregulate pro-apoptotic and anti-proliferative genes in B-cells[33]. Additionally, GR has been shown to translocate to the mitochondria in other systems[34-36], including in thymocytes, where this translocation is associated with glucocorticoid sensitivity[37-39]. This raises the possibility that GR helps induce B-ALL cell death in a non-genomic way, although the impact of GR phosphorylation is unknown.

These findings provide a rationale for the therapeutic use of PI3Kδ inhibitors in combination with glucocorticoids for patients with B-ALL. First, targeting glucocorticoid potentiation to B-ALL cells through the leukocyte-restricted PI3Kδ will likely not increase off-tumor effects. Second, the combination can be highly synergistic in patients with less glucocorticoid sensitive disease and poorer outcomes[10,40,41]. For these patients, PI3Kδ inhibitors could be added to glucocorticoid therapy after the initial glucocorticoid response and cytogenetics are known. Third, because the combination is most synergistic as the glucocorticoid concentration approaches the EC50, glucocorticoid efficacy might be maintained over a longer period while the glucocorticoid is metabolized. Lastly, specific enhancement of glucocorticoid potency opens the door to dose reduction in glucocorticoid-sensitive B-ALL, reducing the impact of debilitating off-tumor effects of glucocorticoids.

ACKNOWLEDGEMENTS

The authors acknowledge the work of Maria Nunez Hernandez, who performed the ERK2 phosphorylation experiments in this manuscript but was unable to be contacted to approve submission as a co-author. This work was supported by the NSF (MCB-1552862, MAP), NIH-NICHD (K12HD027748, JAOZ), NCI (P30CA086862, JAOZ), Children's Miracle Network/University of Iowa Dance Marathon (JAOZ), and Aiming for a Cure Foundation (JAOZ, MAP). The Genomics Division of the Iowa Institute of Human Genetics and the Flow Cytometry Facility are supported by the University of Iowa Holden Comprehensive Cancer Center (NCI, P30CA086862), and Iowa City Veteran's Administration Medical Center. The University of Iowa Proteomic facility is supported by an endowment from the Carver Foundation, directed by Dr. R. Marshall Pope. The content is solely the responsibility of the authors and does not necessarily represent the official views of the National Institutes of Health.

AUTHORSHIP

Contributions: JAOZ and MAP prepared the manuscript. All authors performed experiments and analyzed data. JAOZ obtained patient specimens and information. All authors edited and approved the manuscript.

Conflict of interest disclosure: JAOZ discloses spouse employment at Integrated DNA Technologies. The remaining authors declare no competing financial interests.

REFERENCES

1. National Cancer Institute. SEER Cancer Stat Facts: Childhood Leukemia. Vol. 2021; 2021.

2. Dordelmann M, Reiter A, Borkhardt A, et al. Prednisone response is the strongest predictor of treatment outcome in infant acute lymphoblastic leukemia. *Blood*. 1999;94(4):1209-1217.
3. Schrappe M, Arico M, Harbott J, et al. Philadelphia chromosome-positive (Ph+) childhood acute lymphoblastic leukemia: good initial steroid response allows early prediction of a favorable treatment outcome. *Blood*. 1998;92(8):2730-2741.
4. Toscan CE, Jing D, Mayoh C, Lock RB. Reversal of glucocorticoid resistance in paediatric acute lymphoblastic leukaemia is dependent on restoring BIM expression. *Br J Cancer*. 2020.
5. Xiao H, Ding Y, Gao Y, et al. Haploinsufficiency of NR3C1 drives glucocorticoid resistance in adult acute lymphoblastic leukemia cells by down-regulating the mitochondrial apoptosis axis, and is sensitive to Bcl-2 blockage. *Cancer Cell Int*. 2019;19:218.
6. Kruth KA, Fang M, Shelton DN, et al. Suppression of B-cell development genes is key to glucocorticoid efficacy in treatment of acute lymphoblastic leukemia. *Blood*. 2017;129(22):3000-3008.
7. de Vries MAG, van Litsenburg RRL, Huisman J, et al. Effect of dexamethasone on quality of life in children with acute lymphoblastic leukaemia: a prospective observational study. *Health and Quality of Life Outcomes*. 2008;6(1):103.
8. Pound CM, Clark C, Ni A, Athale U, Lewis V, Halton JM. Corticosteroids, Behavior, and Quality of Life in Children Treated for Acute Lymphoblastic Leukemia; A Multicentered Trial. *J Pediatr Hematol Oncol*. 2012;34(7):517-523.
9. Robison LL. Late effects of acute lymphoblastic leukemia therapy in patients diagnosed at 0-20 years of age. *Hematology Am Soc Hematol Educ Program*. 2011;2011:238-242.
10. Poulard C, Kim HN, Fang M, et al. Relapse-associated AURKB blunts the glucocorticoid sensitivity of B cell acute lymphoblastic leukemia. *Proc Natl Acad Sci U S A*. 2019.
11. Chantry D, Vojtek A, Kashishian A, et al. p110delta, a novel phosphatidylinositol 3-kinase catalytic subunit that associates with p85 and is expressed predominantly in leukocytes. *J Biol Chem*. 1997;272(31):19236-19241.
12. Ismaili N, Garabedian MJ. Modulation of glucocorticoid receptor function via phosphorylation. *Ann N Y Acad Sci*. 2004;1024:86-101.
13. Chen W, Dang T, Blind RD, et al. Glucocorticoid receptor phosphorylation differentially affects target gene expression. *Mol Endocrinol*. 2008;22(8):1754-1766.
14. Treviño LS, Weigel NL. Phosphorylation: a fundamental regulator of steroid receptor action. *Trends Endocrinol Metab*. 2013;24(10):515-524.
15. Jones CL, Gearheart CM, Fosmire S, et al. MAPK signaling cascades mediate distinct glucocorticoid resistance mechanisms in pediatric leukemia. *Blood*. 2015;126(19):2202-2212.
16. Ianevski A, Giri AK, Aittokallio T. SynergyFinder 2.0: visual analytics of multi-drug combination synergies. *Nucleic Acids Res*. 2020;48(W1):W488-W493.
17. Love MI, Huber W, Anders S. Moderated estimation of fold change and dispersion for RNA-seq data with DESeq2. *Genome Biol*. 2014;15(12):550.
18. Risso D, Ngai J, Speed TP, Dudoit S. Normalization of RNA-seq data using factor analysis of control genes or samples. *Nat Biotechnol*. 2014;32(9):896-902.
19. Zhang L, Martini GD, Rube HT, et al. SelexGLM differentiates androgen and glucocorticoid receptor DNA-binding preference over an extended binding site. *Genome Res*. 2018;28(1):111-121.
20. Khokhlatchev A, Xu S, English J, Wu P, Schaefer E, Cobb MH. Reconstitution of mitogen-activated protein kinase phosphorylation cascades in bacteria. Efficient synthesis of active protein kinases. *J Biol Chem*. 1997;272(17):11057-11062.
21. Ishihama Y, Rappsilber J, Mann M. Modular stop and go extraction tips with stacked disks for parallel and multidimensional Peptide fractionation in proteomics. *J Proteome Res*. 2006;5(4):988-994.

22. Yu CL, Summers RM, Li Y, Mohanty SK, Subramanian M, Pope RM. Rapid Identification and Quantitative Validation of a Caffeine-Degrading Pathway in Pseudomonas sp. CES. *J Proteome Res*. 2015;14(1):95-106.
23. Brinkman EK, van Steensel B. Rapid Quantitative Evaluation of CRISPR Genome Editing by TIDE and TIDER. *Methods Mol Biol*. 2019;1961:29-44.
24. Kaspers GJ, Pieters R, Van Zantwijk CH, Van Wering ER, Van Der Does-Van Den Berg A, Veerman AJ. Prednisolone resistance in childhood acute lymphoblastic leukemia: vitro-vivo correlations and cross-resistance to other drugs. *Blood*. 1998;92(1):259-266.
25. Shojaee S, Caeser R, Buchner M, et al. Erk Negative Feedback Control Enables Pre-B Cell Transformation and Represents a Therapeutic Target in Acute Lymphoblastic Leukemia. *Cancer Cell*. 2015;28(1):114-128.
26. Li LB, Goleva E, Hall CF, Ou LS, Leung DY. Superantigen-induced corticosteroid resistance of human T cells occurs through activation of the mitogen-activated protein kinase kinase/extracellular signal-regulated kinase (MEK-ERK) pathway. *J Allergy Clin Immunol*. 2004;114(5):1059-1069.
27. Wang Z, Garabedian MJ. Modulation of glucocorticoid receptor transcriptional activation, phosphorylation, and growth inhibition by p27Kip1. *J Biol Chem*. 2003;278(51):50897-50901.
28. Blind RD, Garabedian MJ. Differential recruitment of glucocorticoid receptor phospho-isoforms to glucocorticoid-induced genes. *J Steroid Biochem Mol Biol*. 2008;109(1-2):150-157.
29. Larsen EC, Devidas M, Chen S, et al. Dexamethasone and High-Dose Methotrexate Improve Outcome for Children and Young Adults With High-Risk B-Acute Lymphoblastic Leukemia: A Report From Children's Oncology Group Study AALL0232. *J Clin Oncol*. 2016;34(20):2380-2388.
30. Unal EB, Uhlitz F, Bluthgen N. A compendium of ERK targets. *FEBS Lett*. 2017;591(17):2607-2615.
31. Korfi K, Smith M, Swan J, Somervaille TC, Dhomen N, Marais R. BIM mediates synergistic killing of B-cell acute lymphoblastic leukemia cells by BCL-2 and MEK inhibitors. *Cell Death Dis*. 2016;7(4):e2177.
32. Yasuda T, Hayakawa F, Kurahashi S, et al. B cell receptor-ERK1/2 signal cancels PAX5-dependent repression of BLIMP1 through PAX5 phosphorylation: a mechanism of antigen-triggering plasma cell differentiation. *J Immunol*. 2012;188(12):6127-6134.
33. Yusuf I, Zhu X, Kharas MG, Chen J, Fruman DA. Optimal B-cell proliferation requires phosphoinositide 3-kinase-dependent inactivation of FOXO transcription factors. *Blood*. 2004;104(3):784-787.
34. Kokkinopoulou I, Moutsatsou P. Mitochondrial Glucocorticoid Receptors and Their Actions. *Int J Mol Sci*. 2021;22(11).
35. Moutsatsou P, Psarra AMG, Tsiapara A, Paraskevakou H, Davaris P, Sekeris CE. Localization of the Glucocorticoid Receptor in Rat Brain Mitochondria. *Arch Biochem Biophys*. 2001;386(1):69-78.
36. Scheller K, Sekeris CE, Krohne G, Hock R, Hansen IA, Scheer U. Localization of glucocorticoid hormone receptors in mitochondria of human cells. *Eur J Cell Biol*. 2000;79(5):299-307.
37. Sionov RV, Cohen O, Kfir S, Zilberman Y, Yefenof E. Role of mitochondrial glucocorticoid receptor in glucocorticoid-induced apoptosis. *J Exp Med*. 2006;203(1):189-201.
38. Prenek L, Boldizsár F, Kugyelka R, et al. The regulation of the mitochondrial apoptotic pathway by glucocorticoid receptor in collaboration with Bcl-2 family proteins in developing T cells. *Apoptosis*. 2017;22(2):239-253.
39. Talabér G, Boldizsár F, Bartis D, et al. Mitochondrial translocation of the glucocorticoid receptor in double-positive thymocytes correlates with their sensitivity to glucocorticoid-induced apoptosis. *Int Immunol*. 2009;21(11):1269-1276.
40. Li B, Brady SW, Ma X, et al. Therapy-induced mutations drive the genomic landscape of relapsed acute lymphoblastic leukemia. *Blood*. 2020;135(1):41-55.

41. Autry RJ, Paugh SW, Carter R, et al. Integrative genomic analyses reveal mechanisms of glucocorticoid resistance in acute lymphoblastic leukemia. *Nat Cancer*. 2020;1(3):329-344.

Sample ID	NCI Risk Group	Karyotype	Fusion Genes Identified (if any)	Cytogenetics Grouping (non-infants/relapse)
MAP010	SR	29,XY,+4,+8,+10,+18,+21[20]		Unfavorable
MAP011	SR	56,XY,+X,+Y,+4,+6,+10,+14,+17,+18,der(19)t(1;19)(q23;p13.3),+21,+21[12]	TCF3::PBX1	Favorable
MAP012	SR	46,XY,t(6;8)(q25;q11.2)[8]		Neutral
MAP013	SR	47,XY,dic(9;20)(p13;q11.2),+10,+21[4]/48,idem,+21[5]/48,idem,+X[3]/49,idem,+X,+21[2]		Neutral
MAP014	HR	46,XX,i(9)(q10),t(12;13)(p13;q12)[23]	ETV6::FLT3	Neutral
MAP015	HR	46,XY,del(9)(p13)x2,der(10)t(9;10)(p22;p15),der(12)t(9;12)(p22;q24.3),dup(16)(q13q11.2)[19]		Neutral
MAP016	SR	46,XY[20]	ETV6::RUNX1	Favorable
MAP017	HR	46,XX,der(2)t(2;9)(p11.2;q13),der(14)t(2;14)(p11.2;q32),dup(21)(q22)iAMP21[11]		Unfavorable
MAP018	N/A (infant)	47,XX,add(2)(q33),der(3)t(3;5)(p26;q11.2),+6,del(10)(q24)[15]	BCR::ABL1	N/A
MAP019	N/A (relapse)	49~50,Y,dup(X)(p11.2p22.1),+dup(X)(p11.2p22.1),t(1;7;5)(q21;p11.2;q11.2),del(6)(q23q27),+8,+9,+10,i(21)(q10),+mar[9]		N/A
MAP020	HR	46,XY,i(7)(q10)[14]	P2RY8::CRLF2	Ph-like
MAP021	HR	46,XY,der(19)t(1;19)(q23;p13.3)[10]	TCF3::PBX1	Neutral
MAP023	HR	46,XX,add(12)(p11.2)[4]	ETV6::RUNX1	Favorable
MAP025	N/A (infant)	48,XX,+X,t(4;11)(q21;q23),+21[17]	KMT2A::AFF1	N/A
MAP031	HR	46,XY,t(7;15)(q22;q13)[18]		Neutral
MAP032	SR	54,XY,+X,+4,+6,+14,+17,+18,+21,+21[13]		Neutral
MAP033	SR	46,XY,dup(21)(q22)iAMP21[4]/46,XY,add(9)(p13),dup(21)(q22)iAMP21[8]		Unfavorable
MAP035	HR	46,XX,t(4;11)(q21;q23)[10]/47,XX,+X,t(4;11)(q21;q23)[6]/47,XX,+X,t(4;11)(q21;q23),del(17)(p11.2)[5]/47,XX,+X,t(4;11)(q21;q23),i(17)(q10)[5]	KMT2A::AFF1	Unfavorable
MAP036	SR	47,XX,+10[4]	ETV6::RUNX1	Favorable
MAP039	SR	46,XY,t(1;3)(p34;q29)[24]	ETV6::RUNX1	Favorable

Table 1. Characteristics of primary patient specimens. SR = standard risk. HR = high risk. Ph-like = Philadelphia chromosome-like ALL.

Figure 1. Prednisolone and idelalisib synergistically induce cell death in B-ALL cell lines and primary patient specimens in vitro. Evaluation of synergy in (**A**) NALM6 cells and (**B**) RS4;11 cells treated with the combination of prednisolone and idelalisib. A Bliss score greater than 10 indicates synergy, 10 to -10 indicates additivity, and less than -10 indicates antagonism. Overall score is at the top of each plot, and the peak Bliss score from the black outlined area is given in the box at the top right corner of each plot. Horizontal dashed line indicates the EC50 for prednisolone. (**C**) Response of primary specimens by EC50 of prednisolone (x-axis) and cell viability fraction at maximum tested dose of prednisolone (10 μM) (y-axis). Specimens with positive end of induction minimal residual disease (MRD) are shown in orange, and specimens with unknown end of induction MRD are in blue. The remaining specimens in black were MRD negative. (**D-E**) Correlations (Pearson coefficient R) of prednisolone AUC for patient specimens, NALM6, and RS4;11 cells with overall Bliss score (**D**) and peak Bliss score (**E**) demonstrate a trend toward decreased prednisolone sensitivity correlating with increased synergy with idelalisib, although neither has a $p \leq 0.05$. (**F-I**) Overall (black bars) and peak (pink bars) Bliss scores for the combination treatment of prednisolone plus idelalisib in; (**F**) NCI standard risk specimens, (**G**) NCI high risk specimens, (**H**) infant specimens, and (**I**) a relapsed specimen do not reveal an association between synergy and risk grouping or cytogenetic features. Cytogenetic features of these specimens are favorable/fav (*ETV6::RUNX1* or double trisomy), unfavorable/unfav (*KMT2A* rearrangement, iAMP21, or hypodiploidy), Ph-like (*P2RY8::CRLF2*), or neutral (all other cytogenetic features).

Figure 2. Idelalisib enhances dexamethasone regulation of effector genes in NALM6 cells. (**A**) The numbers of genes up- and down-regulated ($p \leq 0.01$) for NALM6 cells treated with combinations of dexamethasone (dex) and idelalisib (idela) for 24 hours. (**B**) The log2 fold change in genes regulated by 5 nM dexamethasone is enhanced by idelalisib (left), whereas the enhancement by idelalisib at 50 nM dexamethasone is less pronounced for most genes. The linear regression fit is a black line compared to the red line which would be no effect. (**C**) Box plots of up-regulation (left) and down-regulation (right) by 5 nM dexamethasone show significantly enhanced regulation by the addition of idelalisib. (**D**) Plot of the effect of each gene on dex-sensitivity (x-axis) versus regulation by 50 nM dexamethasone (y-axis). Positive effector (purple) and negative effector (green) genes are those whose regulation contributes to dex-induced NALM6 cell death, whereas buffering genes (yellow) oppose dex-induced cell death. (**E**) The log2 fold change of effector genes in response to combinations of dexamethasone and idelalisib. In 2B and 2C, R = Pearson Correlation coefficient. The concentration of idelalisib used in all the experiments was 250 nM.

Figure 3. Idelalisib enhances prednisolone-induced gene regulation in primary patient specimens.

(**A**) Overall number of genes upregulated (red) and downregulated (blue) in five glucocorticoid-sensitive primary patient specimens treated with idelalisib only (idela), prednisolone only (pred), prednisolone + idelalisib (pred+idela), dexamethasone only (dex), or dexamethasone + idelalisib (dex+idela). (**B**) Comparison of gene expression with prednisolone (x-axis) versus prednisolone + idelalisib (y-axis) in glucocorticoid-sensitive specimens. (**C-D**) Overall number of genes regulated in (**C**) two primary patient specimens with an additive response (MAP014 Bliss score 3 and MAP031 Bliss score -5) and (**D**) two primary patient specimens with a synergistic response (MAP015 Bliss score 22 and MAP019 Bliss score 14) to combination pred+idela treatment in viability assays at the concentrations used for RNA-seq. (**E-F**)

Comparison of gene expression with (**E**) dexamethasone only or (**F**) prednisolone only in primary patient specimens with additive (x-axis) vs. synergistic (y-axis) responses to pred+idela treatment in viability assays. (**G-H**) Comparison of gene expression with dexamethasone only (x-axis) versus dexamethasone plus idelalisib (y-axis) in (**G**) primary patient specimens with an additive response or (**H**) with a synergistic response to pred+idela treatment in viability assays. (**I-J**) Comparison of gene expression with prednisolone only (x-axis) versus prednisolone plus idelalisib (y-axis) in (**I**) primary patient specimens with an additive response or (**J**) with a synergistic response to pred+idela treatment in viability assays. For all scatterplots, Pearson correlation and regression equations are reported.

Figure 4. Phosphorylation of GR at S226 inhibits DNA binding. (**A**) Purified GR-AF1-DBD was expressed and phosphorylated with ERK2. Phosphorylated species of GR-AF1-DBD were separated by strong anion exchange, isolating species with primarily one (1P) and six (6P) phosphates. (**B**) Size exclusion chromatography indicated that unmodified GR (black) eluted at a lower volume than two independent samples of GR-AF1-DBD-1P (blue, green). (**C**) Mass spectrometry of phosphorylated GR-AF1-DBD-6P maps phosphorylation at six residues after ERK2 phosphorylation and isolation of GR-6P, including S203, with S226 being the most prevalent. (**D**) Unmodified GR-AF1-DBD binds with higher affinity than 6P, but when GR-1P (S226P) binding is more strongly inhibited. Dissociation constants (K_D) were measured by electrophoretic mobility shift assays. Adjusted p-values for one-way ANOVA are 0.0036 (***) and <0.0001 (****).

Figure 5. Decreased phosphorylation of GR at S203 or S226 increases glucocorticoid sensitivity. (**A**) Western blots illustrating phosphorylated S203 (top panel) and S226 (bottom panel) of GR in NALM6 cells treated with vehicle, dexamethasone (Dex) only, idelalisib (Idela) only, and dexamethasone with idelalisib (Dex+Idela) for 24 hours. For S226, both low dose dexamethasone (5 nM, left) and high dose dexamethasone (1 µM, right) were used. (**B**) Quantification of GR as the ratio of phosphorylated S203 to total GR normalized to vehicle control. The difference between 5 nM Dex and 5 nM Dex with idelalisib was not statistically significant ($p = 0.36$). (**C**) Quantification of GR as the ratio of phosphorylated S226 to total GR normalized to vehicle control. Phosphorylation of S226 is significantly reduced with both 1 µM Dex ($p = 0.02$) and 250 nM Idela ($p = 0.01$) compared to a theoretical mean of 1. (**D**) EC50 of prednisolone for 2 CRISPR mutants with GR S203A (C11 and D7) compared to wild-type (WT) Nalm6 cells, 3 replicates per cell type. Adjusted p-values for one-way ANOVA are 0.0029 (**) and 0.0007 (***). (**E**) EC50 of prednisolone for 3 CRISPR mutants with GR S226A (B9, B11, C3) compared to wild-type (WT) Nalm6 cells, 6 replicates per cell type. Adjusted p-values for one-way ANOVA are 0.02 (*) and <0.001 (***). (**F-G**) Representative Bliss synergy plots for (**F**) the C11 mutant with GR S203A tested with prednisolone and idelalisib and (**G**) the C3 mutant with GR S226A tested with prednisolone and idelalisib. The peak Bliss score area is outlined by the black rectangle on each synergy plot, with that score given in the box to the right. The EC50 of prednisolone for each CRISPR mutant is indicated by the horizontal dashed line, demonstrating that peak synergy occurs around the prednisolone EC50. The S203A mutation appears to shift the peak synergy to a lower dose of idelalisib while the S226A mutation decreases the overall Bliss synergy score in comparison to wild-type NALM6 cells.

Figure 6. Proposed model of idelalisib-induced glucocorticoid potentiation. Created with BioRender.com.

Figure 1

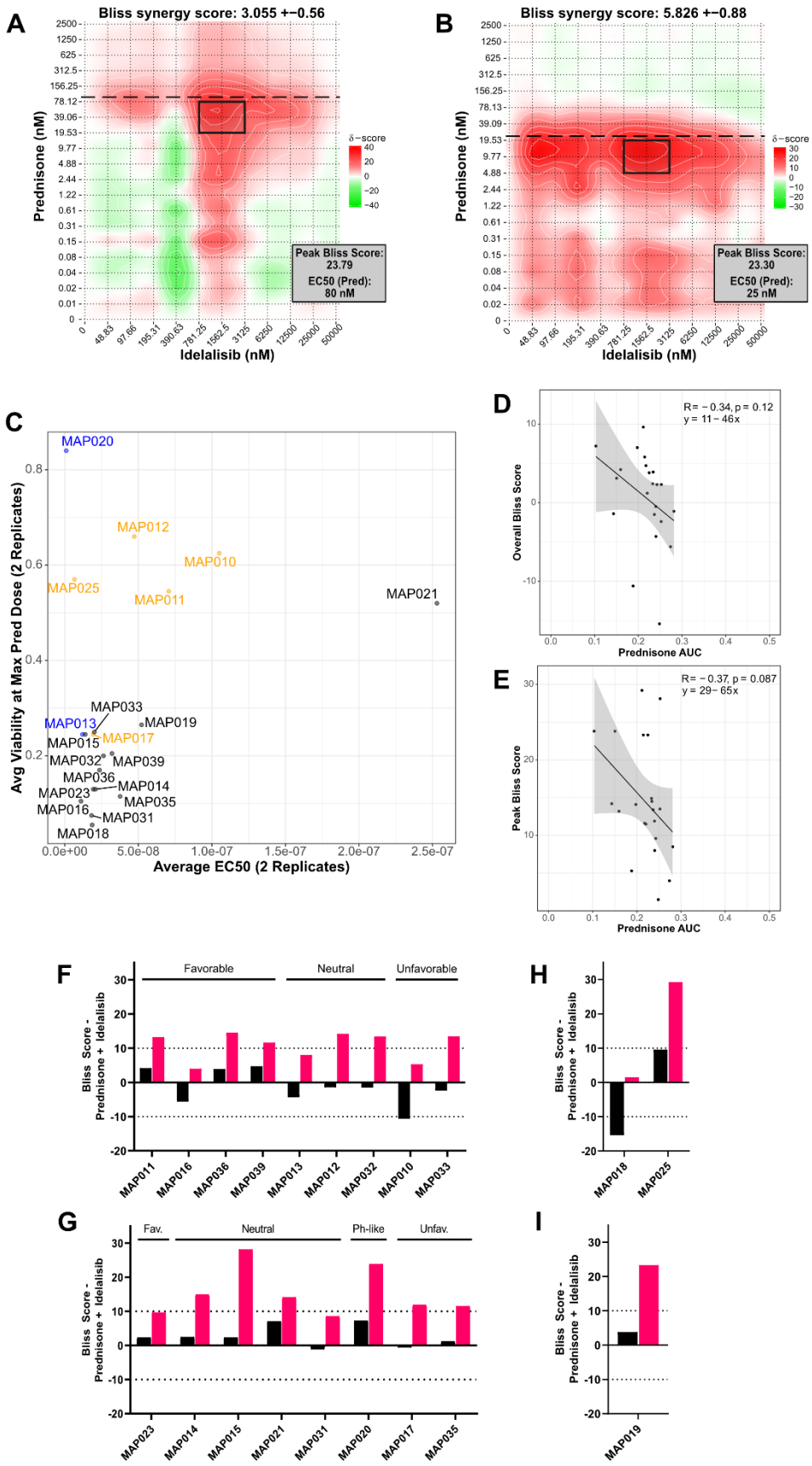
A
Bliss synergy score: 3.055 +−0.56
Prednisone (nM)
Idelalisib (nM)
δ−score
Peak Bliss Score: 23.79
EC50 (Pred): 80 nM
B
Bliss synergy score: 5.826 +−0.88
Prednisone (nM)
Idelalisib (nM)
δ−score
Peak Bliss Score: 23.30
EC50 (Pred): 25 nM
C
Avg Viability at Max Pred Dose (2 Replicates)
Average EC50 (2 Replicates)
MAP020
MAP012
MAP010
MAP025
MAP011
MAP021
MAP033
MAP019
MAP013
MAP017
MAP015
MAP032
MAP039
MAP036
MAP014
MAP023
MAP035
MAP016
MAP031
MAP018
D
R= −0.34, p = 0.12
y = 11 − 46x
Overall Bliss Score
Prednisone AUC
E
R= −0.37, p = 0.087
y = 29− 65x
Peak Bliss Score
Prednisone AUC
F
Favorable
Neutral
Unfavorable
Bliss Score - Prednisone + Idelalisib
MAP011
MAP016
MAP036
MAP039
MAP013
MAP012
MAP032
MAP010
MAP033
H
Bliss Score - Prednisone + Idelalisib
MAP018
MAP025
G
Fav.
Neutral
Ph-like
Unfav.
Bliss Score - Prednisone + Idelalisib
MAP023
MAP014
MAP015
MAP021
MAP031
MAP020
MAP017
MAP035
I
Bliss Score - Prednisone + Idelalisib
MAP019

Figure 2

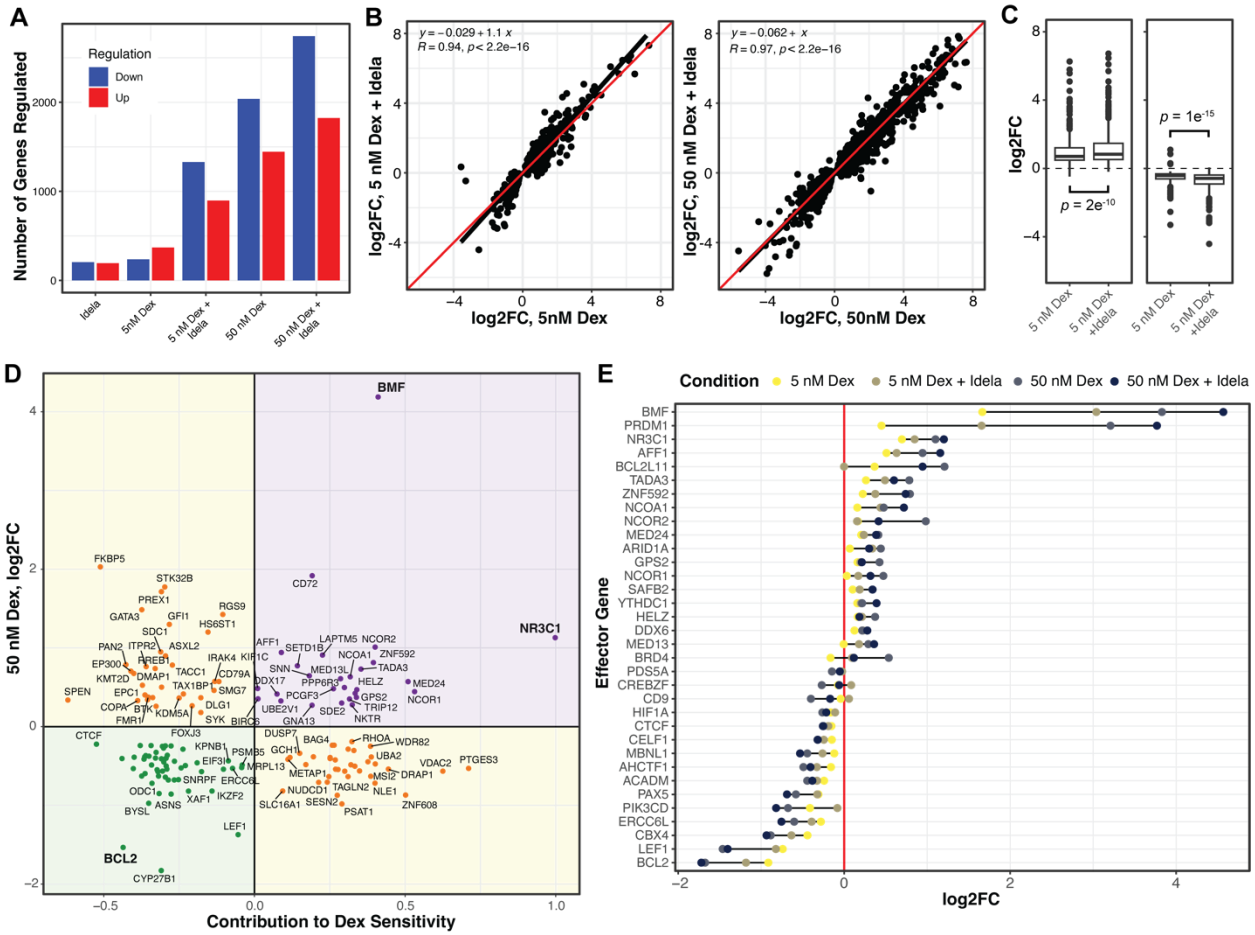
A
Regulation
Down
Up
Number of Genes Regulated
Idela
5nM Dex
5 nM Dex + Idela
50 nM Dex
50 nM Dex + Idela
B
y = −0.029 + 1.1 x
R = 0.94, p < 2.2e−16
log2FC, 5 nM Dex + Idela
log2FC, 5nM Dex
y = −0.062 + x
R = 0.97, p < 2.2e−16
log2FC, 50 nM Dex + Idela
log2FC, 50nM Dex
C
log2FC
p = 1e-15
p = 2e-10
5 nM Dex
5 nM Dex +Idela
D
BMF
NR3C1
BCL2
50 nM Dex, log2FC
Contribution to Dex Sensitivity
E
Condition
5 nM Dex
5 nM Dex + Idela
50 nM Dex
50 nM Dex + Idela
Effector Gene
log2FC

Figure 3

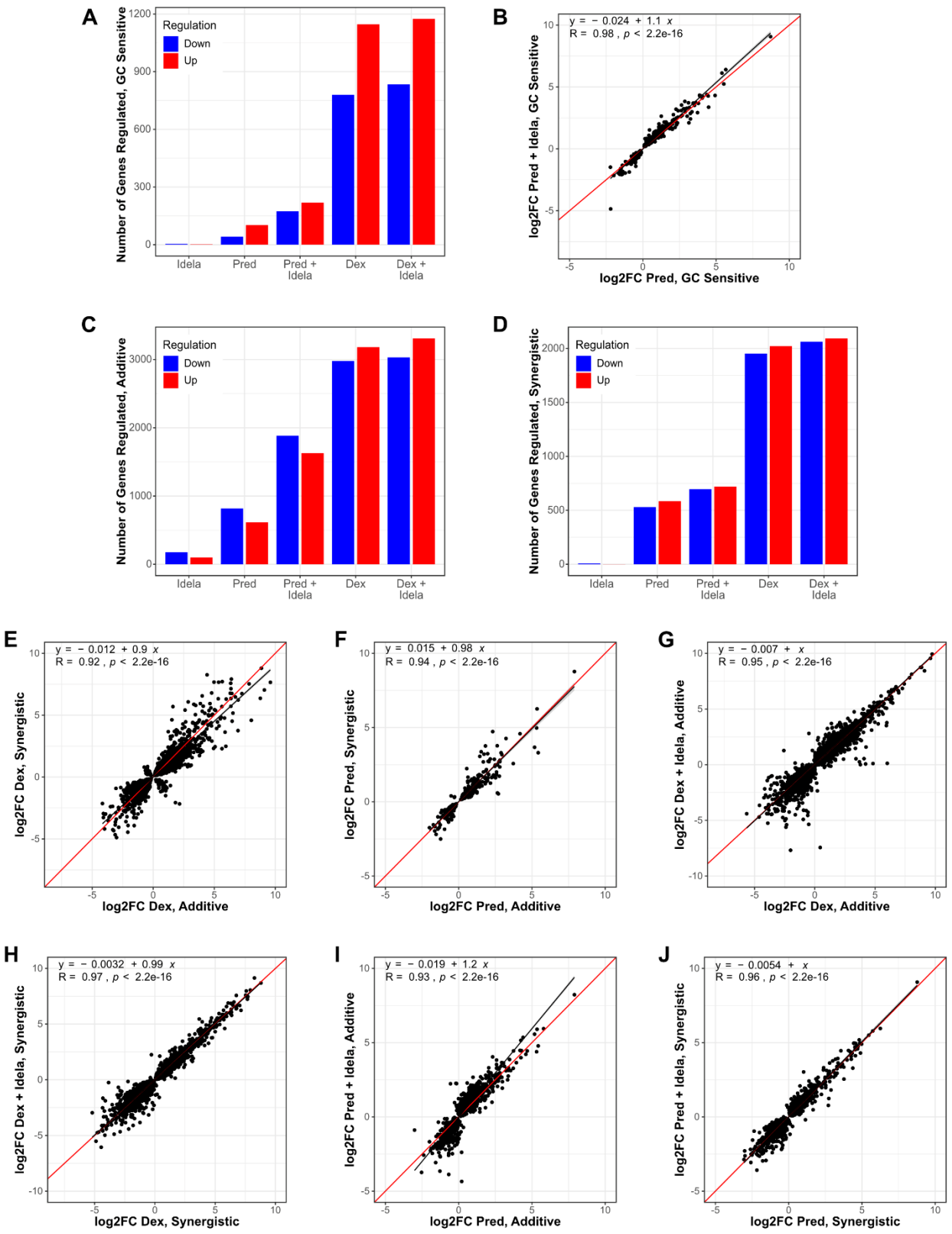
A
Number of Genes Regulated, GC Sensitive
Regulation
Down
Up
Idela
Pred
Pred + Idela
Dex
Dex + Idela
B
y = − 0.024 + 1.1 x
R = 0.98 , p < 2.2e-16
log2FC Pred + Idela, GC Sensitive
log2FC Pred, GC Sensitive
C
Number of Genes Regulated, Additive
D
Number of Genes Regulated, Synergistic
E
y = − 0.012 + 0.9 x
R = 0.92 , p < 2.2e-16
log2FC Dex, Synergistic
log2FC Dex, Additive
F
y = 0.015 + 0.98 x
R = 0.94 , p < 2.2e-16
log2FC Pred, Synergistic
log2FC Pred, Additive
G
y = − 0.007 + x
R = 0.95 , p < 2.2e-16
log2FC Dex + Idela, Additive
log2FC Dex, Additive
H
y = − 0.0032 + 0.99 x
R = 0.97 , p < 2.2e-16
log2FC Dex + Idela, Synergistic
log2FC Dex, Synergistic
I
y = − 0.019 + 1.2 x
R = 0.93 , p < 2.2e-16
log2FC Pred + Idela, Additive
log2FC Pred, Additive
J
y = − 0.0054 + x
R = 0.96 , p < 2.2e-16
log2FC Pred + Idela, Synergistic
log2FC Pred, Synergistic

Figure 4

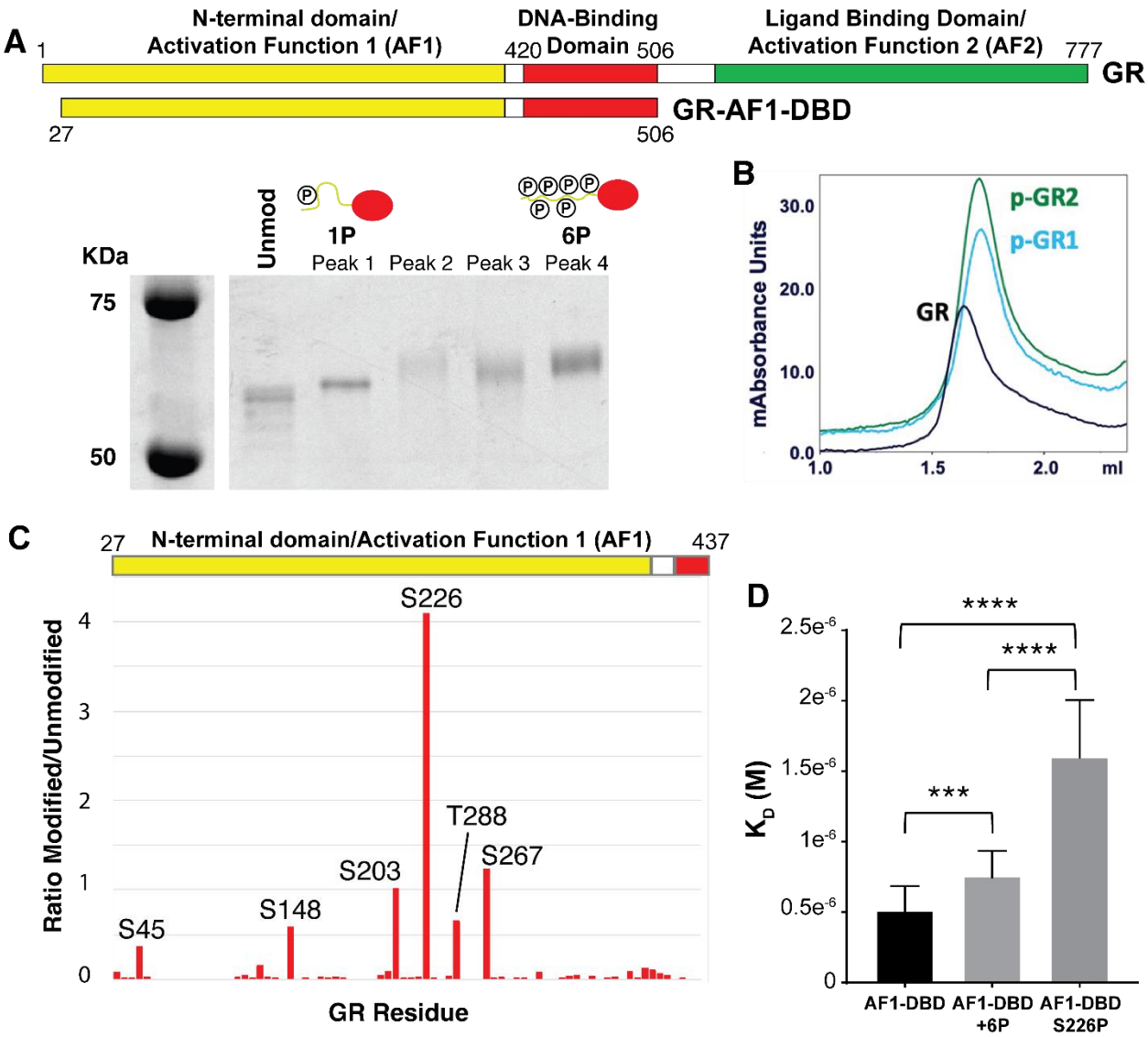
A
N-terminal domain/
Activation Function 1 (AF1)
DNA-Binding
Domain
Ligand Binding Domain/
Activation Function 2 (AF2)
1
420
506
777
GR
GR-AF1-DBD
27
506
KDa
75
50
Unmod
1P
6P
Peak 1
Peak 2
Peak 3
Peak 4
B
mAbsorbance Units
30.0
20.0
10.0
0.0
1.0
1.5
2.0
ml
p-GR2
p-GR1
GR
C
27
N-terminal domain/Activation Function 1 (AF1)
437
Ratio Modified/Unmodified
4
3
2
1
0
S226
T288
S267
S203
S148
S45
GR Residue
D
K_D (M)
2.5e-6
2e-6
1.5e-6
1e-6
0.5e-6
0
****
****
***
AF1-DBD
AF1-DBD +6P
AF1-DBD S226P

Figure 5

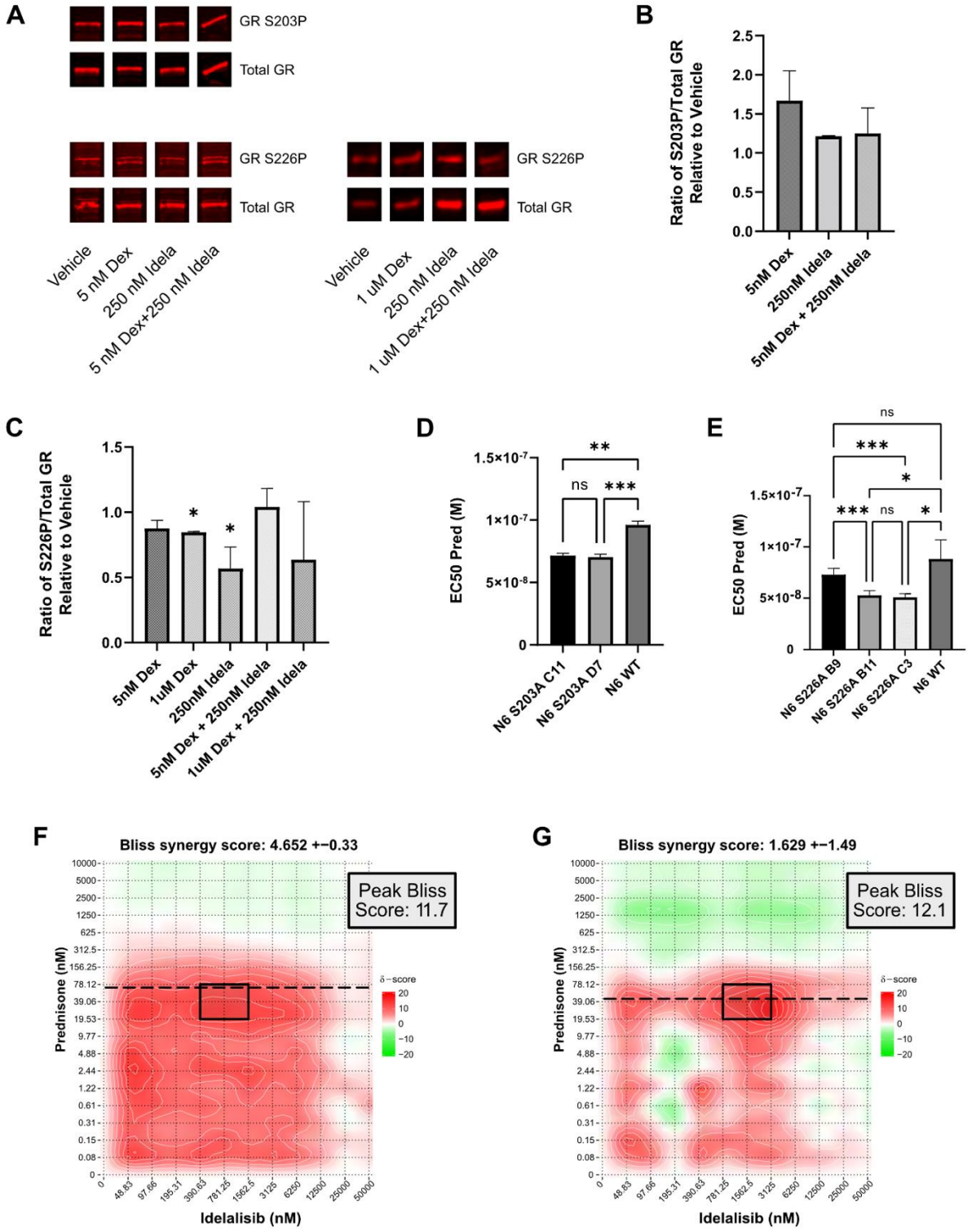
A
GR S203P
Total GR
GR S226P
Total GR
GR S226P
Total GR
Vehicle
5 nM Dex
250 nM Idela
5 nM Dex+250 nM Idela
Vehicle
1 uM Dex
250 nM Idela
1 uM Dex+250 nM Idela
B
Ratio of S203P/Total GR Relative to Vehicle
5nM Dex
250nM Idela
5nM Dex + 250nM Idela
C
Ratio of S226P/Total GR Relative to Vehicle
5nM Dex
1uM Dex
250nM Idela
5nM Dex + 250nM Idela
1uM Dex + 250nM Idela
D
EC50 Pred (M)
N6 S203A C11
N6 S203A D7
N6 WT
E
EC50 Pred (M)
N6 S226A B9
N6 S226A B11
N6 S226A C3
N6 WT
F
Bliss synergy score: 4.652 +−0.33
Peak Bliss Score: 11.7
Prednisone (nM)
Idelalisib (nM)
δ−score
G
Bliss synergy score: 1.629 +−1.49
Peak Bliss Score: 12.1
Prednisone (nM)
Idelalisib (nM)
δ−score

Figure 6

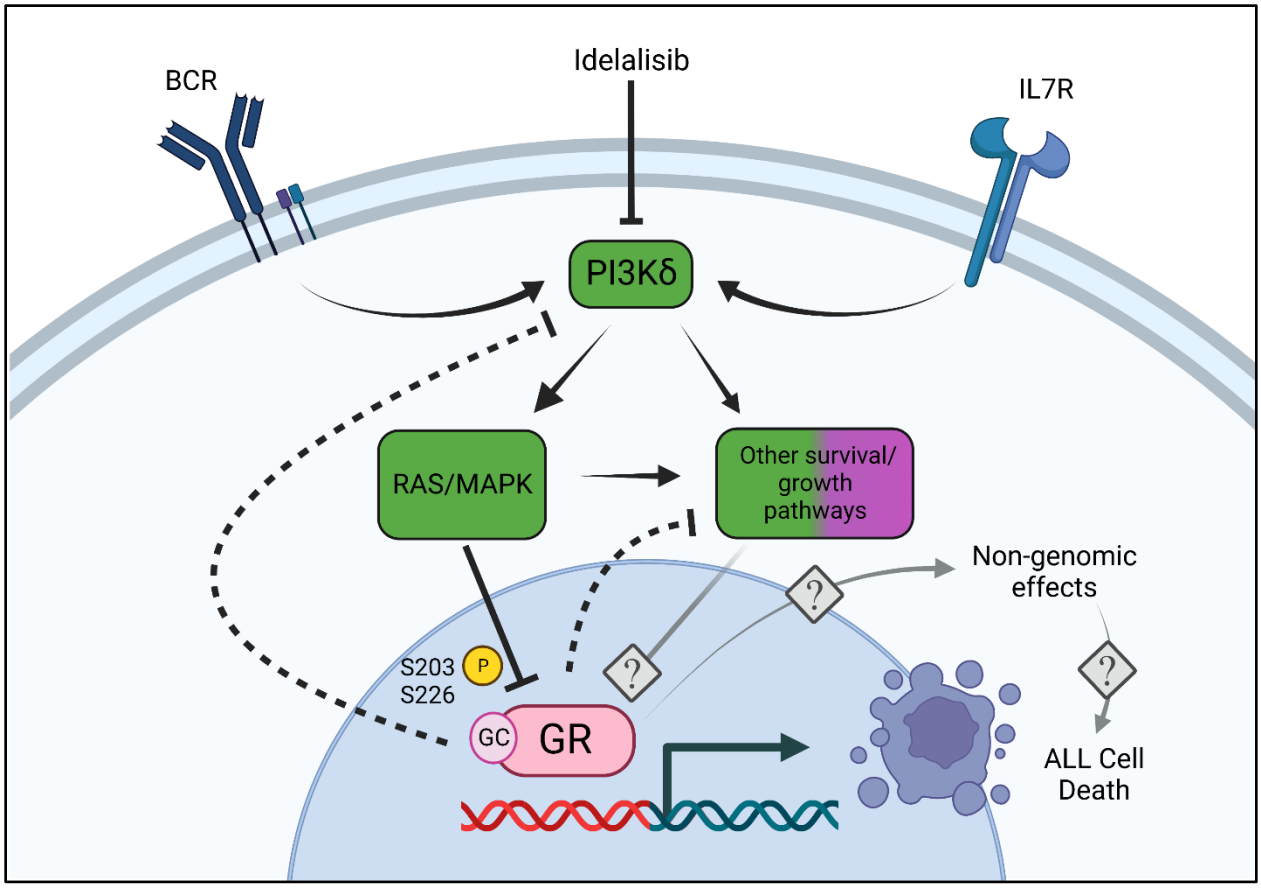
BCR
Idelalisib
IL7R
PI3Kδ
RAS/MAPK
Other survival/
growth
pathways
Non-genomic
effects
S203
S226
P
GC
GR
ALL Cell
Death